Journal of Inclusion Phenomena and Molecular Recognition in Chemistry **13**: 47–61, 1992.

Intercalative Reaction of a Cobalt(III) Cage Complex, $Co(sep)^{3+}$, with Magadiite, a Layered Sodium Silicate

JAMES S. DAILEY and THOMAS J. PINNAVAIA
Department of Chemistry and Center for Fundamental Materials Research, Michigan State University, East Lansing, Michigan 48824, U.S.A.

(Received: 17 May 1991; in final form: 8 August 1991)

Abstract. The cationic metal cage complex (1,3,6,8,10,13,16,19-octaazabicyclo[6.6.6]eicosane)cobalt(III), $Co(sep)^{3+}$, has been investigated as a potential pillaring reagent for Na^+-magadiite ($Na_{1.7}Si_{14}O_{27.9}(OH)_{1.9} \cdot 7.6\,H_2O$) a synthetic layered sodium silicate. Reaction of Na^+-magadiite with aqueous solutions of $Co(sep)Cl_3$ at 25°C resulted in the binding of $Co(sep)^{3+}$ cations to the external crystalline surface of the layered silicate. In contrast, an intercalated product exhibiting a 17.6 Å basal spacing was generated by reaction at 100°C. ^{29}Si MAS NMR and FT-IR spectroscopy indicate that $Co(sep)^{3+}$ intercalated reaction products retain the magadiite layer structure. Moreover, scanning electron micrographs of the reaction products showed retention of the original particle morphology, suggesting a topotactic intercalation. However, during intercalation, some of the $Co(sep)^{3+}$ was found to undergo an unusual demetalation reaction leaving a combination of Co(II) and $Co(sep)^{3+}$ between the layers. Nitrogen surface area analysis showed that only a small amount of microporous surface existed in the $Co(sep)^{3+}$ intercalated derivative, suggesting that most of the interlayer space is 'stuffed' with cobalt species.

Key words. Magadiite, intercalation, cobalt sepulchrate, pillaring reactions, ^{29}Si MAS NMR, N_2 gas adsorption.

1. Introduction

Pillared layered materials have attracted widespread interest recently due in part to their potential utility as catalysts and molecular sieving adsorbents [1, 2]. Normally, pillared microporous solids are derived from materials with ion exchange capabilities. Examples of layered ionic materials that have been examined previously for their pillaring properties include 2:1 phylosilicate clays, layered double hydroxides and zirconium phosphates [1]. Another class of ionic layered minerals, namely the hydrous sodium silicates, have been identified as having intercalation properties suitable for producing pillared derivatives [2]. In an effort to broaden the diversity of pillared materials, we have been investigating the pillaring reactions of lamellar hydrous sodium silicates. Examples of this unique family of silicates include, magadiite ($Na_2Si_{14}O_{29} \cdot 9H_2O$), kenyaite ($Na_2Si_{20}O_{41} \cdot 10H_2O$), and kanemite ($NaHSi_2O_5 \cdot H_2O$). All are naturally occurring minerals first found in lake beds at Lake Magadi, Kenya [3]. These compounds also can be conveniently prepared in the laboratory via hydrothermal synthesis [4–6]. It has been shown that the hydrated interlayer sodium ions of these materials can be exchanged by large alkylammonium cations to form organic derivatives [5–7]. These alkylammonium derivatives of magadiite and kenyaite have been used as precursors for reaction of interlayer silanols by organosilanes [8].

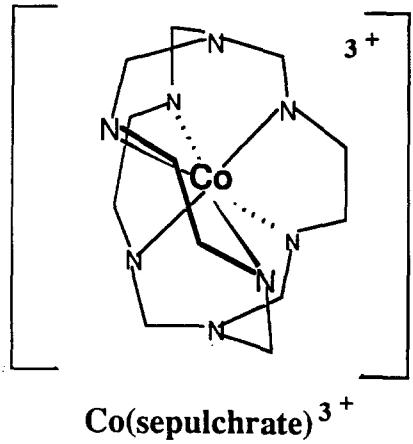

Fig. 1. Schematic representation of the cobalt sepulchrate complex.

Certain alkylammonium exchange forms of smectites show considerable promise as selective adsorbents for the removal of priority pollutants from contaminated ground waters [9, 10]. Similar adsorption properties might be expected for organo-cation exchange forms of layered silicates. However, in contrast to smectite clays, layered sodium silicates have a relatively high layer charge and are not easy to swell. The highly charged layers require highly charged cations to induce porosity. No examples of magadiite intercalated by a robust cation of charge 3^+ or larger have been reported previously.

In this work, we examine the possibility of preparing a pillared derivative of magadiite using a high charged cation of known dimension. The cation chosen for this purpose was cobalt sepulchrate, $[Co(sep)]^{3+}$, a highly stable cobalt cage complex derived from the capping of trisethylenediaminecobalt(III) cation [11]. The structure of this complex is illustrated in Figure 1.

2. Experimental

2.1. PREPARATION OF Na^+-MAGADIITE

Synthetic Na^+-magadiite was prepared by the reaction of NaOH and SiO_2 under hydrothermal conditions according to a previously described method [4]. A suspension of Davisil 62 SiO_2 (12.0 g, 0.20 mol) in 60 mL of 1.11 M NaOH (0.067 mol) was allowed to digest at 150°C for 46 hours in a Teflon-lined stainless steel bomb. The solid Na^+-magadiite reaction product was separated by centrifugation, washed twice with 200 mL of deionized water in order to remove excess NaOH and air dried at 40°C.

2.2. PREPARATION OF $Co(sep)Cl_3$

The synthesis of (1,3,6,8,10,13,16,19-octaazabicyclo[6.6.6]eicosane)cobalt(III) chloride, $[Co(sep)]Cl_3$, was accomplished by using the method described by Creaser *et*

al. [11]. To a stirred suspension of $[Co(en)_3]Cl_3 \cdot H_2O$(18.0 g, 0.05 mol) and Li_2CO_3 (25 g, 0.34 mol) in deionized H_2O (125 mL) were added 37.9% aqueous formaldehyde (550 mL, 7.5 mol) and 30% aqueous NH_4OH (157.4 mL, 2.5 mol diluted to 550 mL). The solutions were added separately by addition funnel over a period of 3 h. The mixture was stirred for an additional 30 min, and Li_2CO_3 was filtered from the red solution. The pH of the filtrate was adjusted from 9 to 2.5 by the addition of concentrated $HClO_4$, and the $LiClO_4$ that formed was filtered from the solution. The filtrate was passed through a Dowex 50W-X8 column (100–200 mesh), and the column was washed with five liters of 0.2 M trisodium citrate. The resin was then washed with water and 1 M HCl to remove Na^+. The resultant orange $Co(sep)^{3+}$ cation was eluted from the column with 3 M HCl ($\approx$ 4L). The orange solution was reduced to dryness on a rotoevaporator and recrystallized from water by the addition of acetone. *Anal. Calcd.* for: $CoC_{12}N_8H_{30}Cl_3$: Co, 13.05; C, 31.91; N, 24.81; H, 6.69; Cl, 23.54. *Found*: Co, 12.41; C, 30.76; N, 23.72; H, 6.96.

2.3. $Co(sep)^{3+}$-MAGADIITE REACTIONS

$Co(sep)^{3+}$ exchange forms of magadiite were prepared by the addition of synthetic Na^+-magadiite (0.50 g, 4.7×10^{-4} mol) in 10 mL of deionized water to $Co(sep)Cl_3$ (0.914 g, 2.02×10^{-3} mol) in water (40 mL). Reaction mixtures were maintained either at 25°C for 72 h or at 100°C for 24 h. After each reaction period, the solid was centrifuged and reexchanged with 50 mL of fresh 0.04 M $Co(sep)Cl_3$ solution. The exchange solutions were replaced up to four times. Each reaction product was recovered by centrifugation and washed with deionized water until the orange solid was Cl^- free.

2.4. PHYSICAL MEASUREMENTS

Basal spacings were determined from 001 X-ray reflections using a Rigaku Rotaflex diffractometer equipped with CuKα radiation. Samples were prepared by depositing a suspension of the washed solid on a glass microscope slide and allowing the suspension to air dry at 40°C. The extent of intercalation was followed after each exchange by measuring the change in basal spacing.

^{29}Si MAS NMR experiments were performed on a Varian 400 VXR solid state NMR spectrometer operated at 79.5 MHz. A Doty multinuclear MAS probe equipped with zirconia rotors was used for all measurements. ^{29}Si spin lattice relaxation times were determined experimentally by inversion recovery experiments. The ^{29}Si relaxation time and 90° pulse width for Na-magadiite were found to be 280 seconds and 5.8 μs, respectively. The Q^3 and Q^4 silicon environments exhibited relaxation times of 160 s and 280 s, respectively. A total of 12 scans were recorded for each sample. The sample spinning rate was approximately 5 kHz. A delay time five times as large as T_1 for the Q^4 sites was used in order to obtain quantitative results.

Nitrogen adsorption isotherms at liquid nitrogen temperature were determined on a Quantachrome Quantasorb Jr. using ultrapure nitrogen. Helium was the carrier gas and all samples were outgassed at 120°C under flowing He for 12 h. Surface areas were determined using the BET equation and the t-plot method [12].

FTIR spectra were obtained on an IBM IR44 spectrometer using the KBr pressed pellet technique. All pellets contained 2% sample by weight.

Thermogravimetric analyses were performed using a Cahn TG system 121 analyzer. All samples were heated to 1000°C at a heating rate of 5°C/min.

3. Results and Discussion

3.1. PREPARATION OF Na^+-MAGADIITE

Base hydrolysis of silica gel at 150°C under autogenus pressure produced a well crystallized Na^+-magadiite product. The X-ray diffraction pattern for an air dried film sample, shown in Figure 2, exhibited 001 reflections corresponding to a basal spacing of 15.6 Å. Despite the planar structure of Na^+-magadiite and efforts to produce well oriented films, several *hkl* reflections with $h \neq k \neq 0$ were observed due to the rosette-like morphology of the aggregated platelets. The broad lump in the X-ray pattern centered near 20 degrees 2θ ($d = 4.43$ Å) may be indicative of a

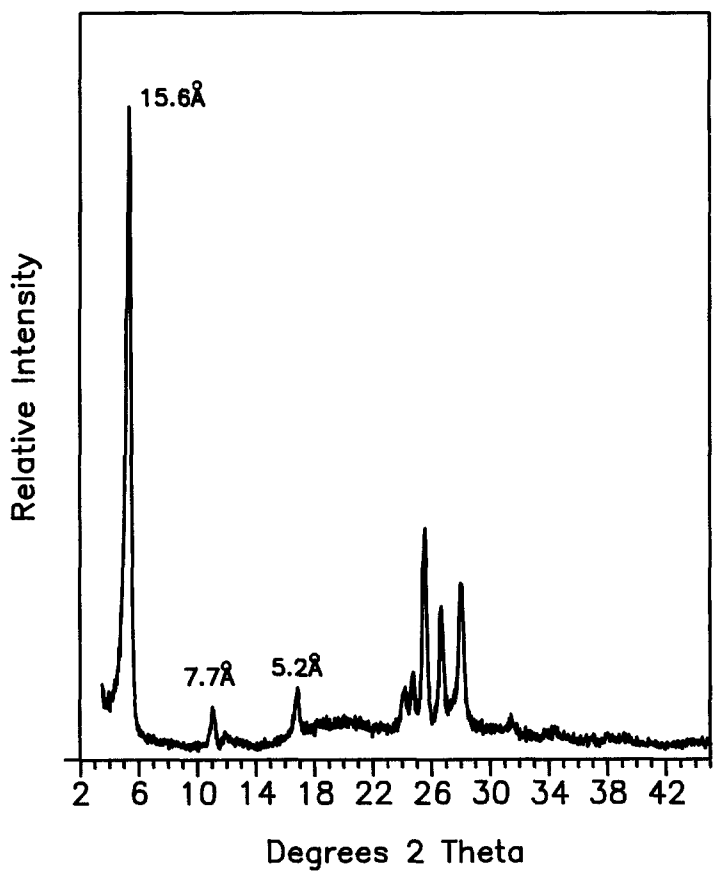

Fig. 2. X-ray diffraction pattern (Cu-K_α) of an oriented film sample of Na^+-magadiite.

quasi-crystalline silica impurity. The peak positions for this synthetic product agreed closely with values reported previously for synthetic and natural magadiite [3, 13–15].

The sodium content of synthetic Na^+-magadiite depended in part on the extent of hydrolysis that occurred during the washing procedure. Initial washes removed excess NaOH associated with the material. However, repeated washes leached Na^+ cations from the interlayer and caused layer hydrolysis. The chemical composition of Na^+-magadiite was obtained by combining the results of thermogravimetric analyses and chemical analyses. Air dried Na^+-magadiite that had been well washed to remove excess NaOH (Figure 3a) lost 13% of its total weight as water below 200°C. An additional 1.6% was lost between 200–1000°C. The weight loss above 200°C was assigned to the dehydroxylation of SiOH groups. The combination of Na_2O content (4.98%) and weight loss provided an empirical composition for synthetic Na^+-magadiite of $Na_{1.7}Si_{14}O_{27.9}(OH)_{1.9}\cdot 7.6\,H_2O$. These data agreed well with those put forth by Lagaly *et al.* [7] and Garces *et al.* [14] that indicated

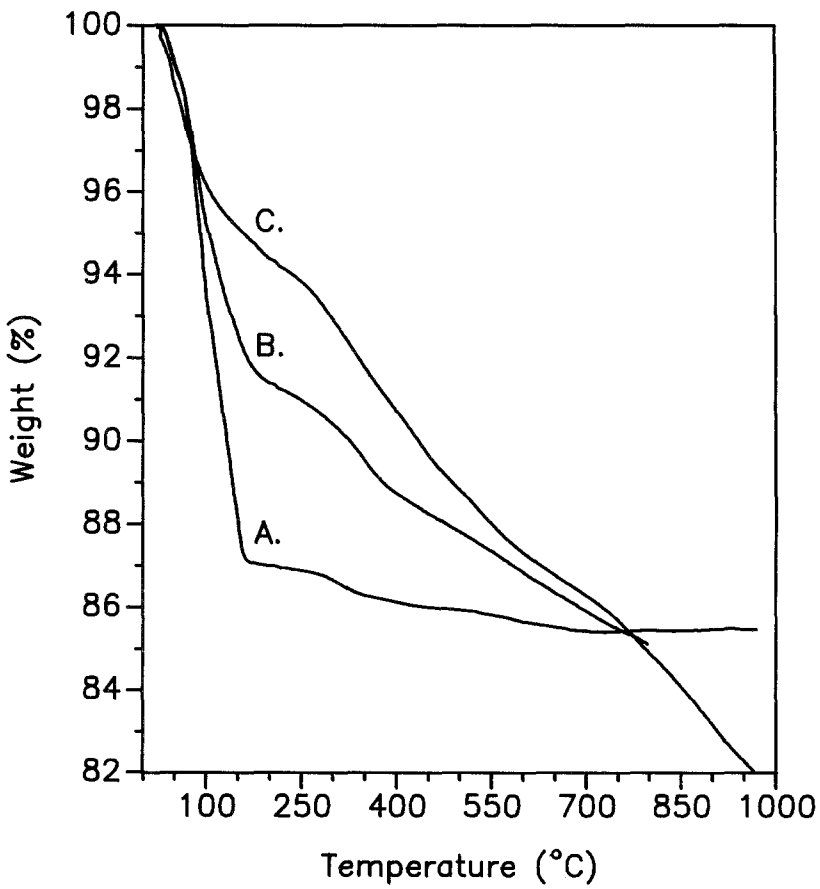

Fig. 3. Thermogravimetric analysis curves obtained under flowing argon for samples (A) Na^+-magadiite, (B) $Co(sep)^{3+}$–mag(25°C) and (C) $Co(sep)^{3+}$–mag(100°C).

Table I. Chemical compositions of natural and synthetic magadiite

Sample	Weight % (mole ratio)				Mole ratio/14 Si		
	Na_2O	SiO_2	H_2O	Total	Na	Si	H_2O
Na^+magadiite, synthetic unwashed, this work	6.58 (1.00)	75.8 (11.9)	15.5 (8.11)	97.88	2.35	14	10.9
Na^+magadiite, synthetic washed, this work	4.98 (1.00)	80.2 (16.6)	14.6 (10.0)	99.78	1.69	14	8.5
Na^+magadiite, synthetic Lagaly (1975)	5.58 (1.00)	74.9 (13.4)	18.2 (3.26)	98.68	2.02	14	11.3
Na^+magadiite, natural McAtee (1968)	5.6 (1.00)	77.4 (13.8)	15.2 (2.71)	98.2	2.13	14	9.2
Na^+magadiite, synthetic Garces (1988)	6.56 (1.00)	84.8 (12.9)	7.8 (1.19)	99.16	2.09	14	4.29
Na^+magadiite, synthetic Garces (1988)	6.31 (1.00)	87.0 (14.2)	8.1 (4.42)	101.4	1.96	14	4.35

an ideal unit cell of $Na_2Si_{14}O_{29}{\cdot}9H_2O$. Other workers report compositions shown in Table 1 that vary between 2.13 and 1.96 sodium cations per 14 silicon atoms. The samples synthesized in this work (cf. Table 1) straddle these compositions, depending on post hydrothermal treatment of the product, especially the number of washings. The water content also varied dramatically depending on differences in drying conditions. The low sodium content of our washed product, 1.69 Na^+ per 14 Si, was a direct result of hydrolysis caused by the extensive washing with water.

3.2. REACTION WITH $Co(sep)^{3+}$

The basal spacings of the products obtained by ion exchange reaction of $Co(sep)^{3+}$ with Na^+-magadiite depended greatly on the reaction temperature. For reactions carried out at 25°C, there is little or no change in the basal spacing of the host material as shown by the XRD patterns in Figure 4. After three treatments with 0.12 N $Co(sep)^{3+}$, the magadiite basal spacing increased slightly from an initial value of 15.6 Å to $\approx$ 15.9 Å. The 001 peak became less symmetric with a possible shoulder developing on the low angle side of the diffraction peak, and the hkl reflections in the region 24–30° 2θ decreased in intensity.

The color of the reaction product obtained at 25°C was orange indicating that some Co complex was bound to the magadiite surface. Despite the change in diffraction pattern and the color change, it was unlikely that significant intercalation had occurred. The change in basal spacing was far too small to be directly attributed to intercalation of $Co(sep)^{3+}$. The change in *hkl* intensities in the 24–30° region most likely were due to breakdown in the rosette morphology of the magadiite as a result of prolonged stirring of the crystals during the exchange reaction. Multiple exchange reactions at 25°C most likely resulted in the $Co(sep)^{3+}$ being bound at the external surfaces of the crystals. Chemical analysis, to be presented below, verified this conclusion.

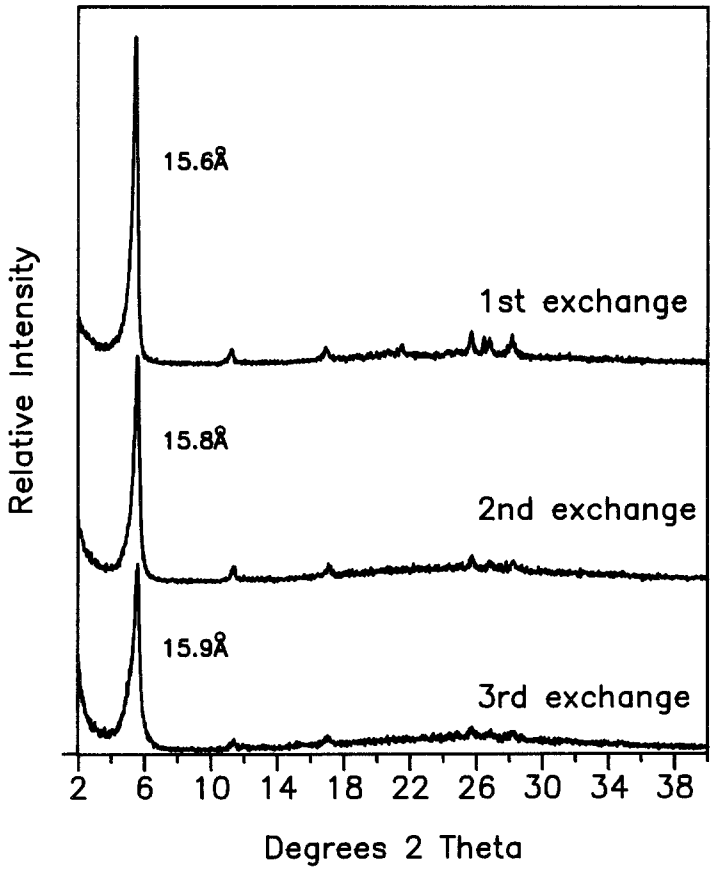

Fig. 4. X-ray diffraction patterns for oriented film samples of the reaction products obtained after successive exchange of Na^+-magadiite with 0.12 N $Co(sep)Cl_3$ at 25°C.

In contrast to the results obtained at 25°C, the successive treatments of Na^+-magadiite with fresh 0.12 N $[Co(sep)]Cl_3$ solutions at 100°C resulted in the steady increase in the basal spacing from 15.6 Å before exchange to 17.6 Å after the 3rd exchange reaction, as shown in Figure 5. Further exchange did not result in additional expansion of the structure. The increase in basal spacing indicated intercalation of $[Co(sep)]^{3+}$ between the layers of magadiite. On the basis of an 11.2 Å thickness for magadiite in the absence of hydrated Na^+ ions, the observed spacing corresponded to a gallery height of ≈ 6.4 Å. This value was in agreement with the gallery height reported for smectite clays pillared by $Ir(diamsar)^{3+}$, an oval-shaped metal cage complex with dimensions similar to $Co(sep)^{3+}$ [16].

The compositions of the products obtained by ion exchange reaction of Na^+-magadiite with $Co(sep)^{3+}$ at 25°C and 100°C were deduced from TGA and chemical analysis. TGA curves for the reaction products produced at 25°C and 100°C, henceforth designated $Co(sep)^{3+}$-Mag(25°C) and $Co(sep)^{3+}$-Mag(100°C), respectively, are shown in Figure 3b and 3c. Included in the figure for comparison purposes are the TGA curves obtained for Na^+-magadiite before exchange with

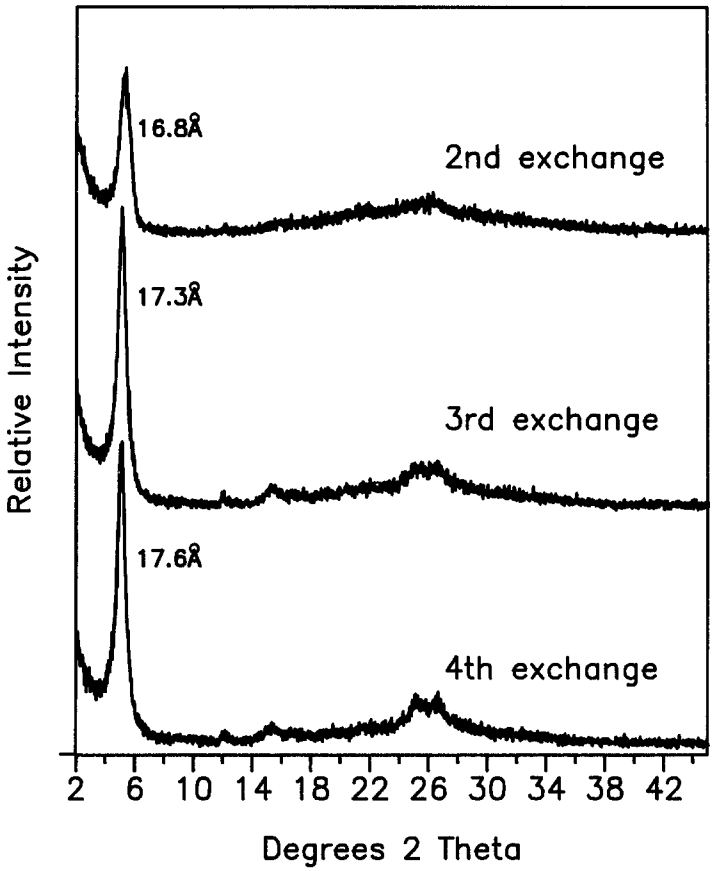

Fig. 5. X-ray diffraction patterns for oriented film samples of the reaction products obtained after successive exchange of Na^+-magadiite with 0.12 N $Co(sep)Cl_3$ at 100°C.

$Co(sep)^{3+}$. The product produced at 25°C exhibited an initial weight loss of 8.5 wt.-% between 20–200°C assigned to adsorbed H_2O. In addition, the 2.0 wt.-% loss from 200–350°C was attributed to dehydroxylation. Above 350°C the weight loss (4.5%) was assigned to the oxidation by air of the sepulchrate ligands of $Co(sep)^{3+}$. Elemental analyses, given in Table II, indicated a total of 4.4 wt.-% carbon and nitrogen, in good agreement with the TGA results.

The product prepared at 100°C exhibited a weight loss of 8.0% below 350°C, which we assigned to the loss of H_2O and hydroxyl groups. The additional 10% weight loss from 350–1000°C was probably due to the loss of sepulchrate ligand by desorption and/or oxidation. Elemental analyses for total carbon and nitrogen was (9.8 wt.-%) in close agreement with the 10% weight loss observed by TGA above 350°C.

On the basis of the data summarized in Table II for $Co(sep)^{3+}$–Mag(25°C), there were approximately 0.18 cobalt atoms per Si_{14} unit. The N/Co molar ratio was 6.63, in reasonable agreement with the expected N/Co molar ratio of 8 for $Co(sep)^{3+}$. A substantially lower N/Co ratio of 4.1 was obtained for $Co(sep)^{3+}$–

Table II. Compositions (wt.-%) of products prepared by reaction of Na^+-magadiite with $Co(sep)^{3+}$ at 25°C and 100°C

	$Co(sep)^{3+}$–Mag(25°C)	$Co(sep)^{3+}$–Mag(100°C)
Na_2O	6.1	0.3
SiO_2	82.7	80.5
Co	1.0	4.2
C	2.7	5.6
H	1.97	2.35
N	1.6	4.2
H_2O[a]	8.5	8.0
Total	102.6	103.3
Chemical formula	A	B

A. $H_{0.46}Na^+_{1.0}[Co(sep)]^{3+}_{0.18}Si_{14}O_{29}\cdot 1.1\ H_2O$.
B. $H_{0.10}Co^{2+}_{0.36}[Co(sep)]^{3+}_{0.39}Si_{14}O_{29}\cdot 1.4\ H_2O$.
[a]Weight loss below 200°C from TGA.

Mag(100°C). The C/N molar ratio was 1.6, in close agreement with the expected C/N molar ratio of 1.5 for $Co(sep)^{3+}$. This suggested that $Co(sep)^{3+}$ cations and uncomplexed cobalt cations were present in this material. Cobalt(II), the most stable uncomplexed form of cobalt in aqueous solution, is known to form a blue complex with SCN^- in ethanolic solution [17]. The supernatant recovered after leaching $Co(sep)^{3+}$–Mag(100°C) with 6 M HCl became deep blue when ethanolic KSCN was added, indicating the presence of Co(II). However, $Co(sep)^{3+}$–Mag(25°C), gave a negative SCN^- test for Co(II), indicating that essentially all the cobalt was bound as the $Co(sep)^{3+}$ complex. Thus, the composition of $Co(sep)^{3+}$–Mag(25°C) was consistent with $Co(sep)^{3+}$ present mainly at the external surfaces of the layered silicate. Whereas $Co(sep)^{3+}$–Mag(100°C) was an authentic intercalation compound that contained a mixture of $Co(sep)^{3+}$ and uncomplexed Co(II), formed as a result of demetalation of $Co(sep)^{3+}$.

The ^{29}Si MAS NMR spectra for Na^+–magadiite, $Co(sep)^{3+}$–Mag(25°C) and $Co(sep)^{3+}$–Mag(100°C) are shown in Figure 6. Na^+–magadiite exhibited two general Si environments, namely Q^3 type $HOSi(OSi)_3$ or $Na^+[OSi(OSi)_3]$ sites and Q^4 type $Si(OSi)_4$ sites [2]. A single Q^3 peak was centered at -99.8 ppm and three Q^4 resonances occurred at -110.7 ppm, -111.7 ppm and -114.2 ppm, respectively. The ratio of integral intensities for Na^+-magadiite, $Q^3/Q^4 = 0.35$, corresponded to 3.63 Q^3 sites/Si_{14}. These data were in close agreement with the Q^3/Si_{14} ratio obtained from the analytical composition ($Q^3/Si_{14} = 3.6$).

The Q^3 and Q^4 resonances in $Co(sep)^{3+}$–Mag(25°C) exhibited chemical shifts similar to those found for Na^+-magadiite, but the lines are somewhat broadened. For instance, the shoulder present at -110.7 ppm in Na^+-magadiite was unresolved in $Co(sep)^{3+}$–Mag(25°C) due to line broadening. The increase in linewidth was even more apparent in $Co(sep)^{3+}$–Mag(100°C). The presence of paramagnetic Co^{2+} in the latter product undoubtedly contributed to the spectral broadening. A comparison of relative integral intensities for the ^{29}Si resonances indicated that the

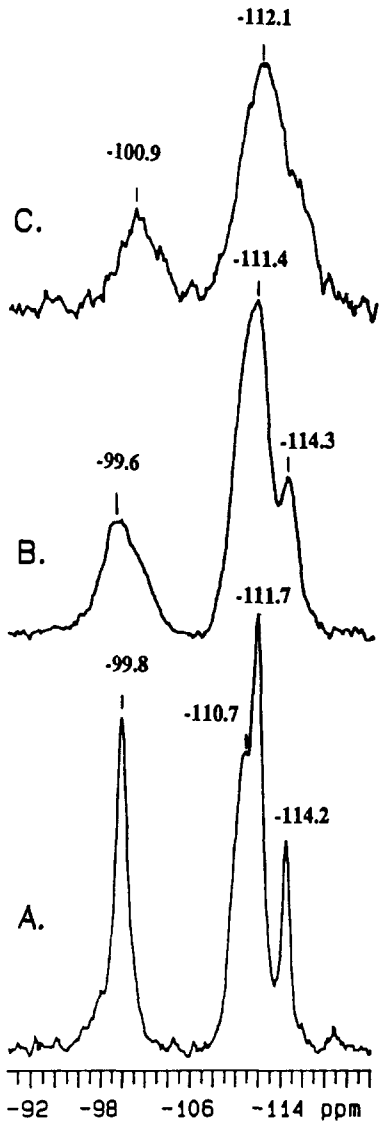

Fig. 6. ^{29}Si Magic Angle Spinning NMR spectra for (A) Na^+-magadiite, (B) $Co(sep)^{3+}$–mag(25°C), and (C) $Co(sep)^{3+}$–mag(100°C).

Q^3/Q^4 ratio was very similar for Na^+-magadiite ($Q^3/Q^4 = 0.35$), $Co(sep)^{3+}$–Mag(25°C) ($Q^3/Q^4 = 0.27$), and $Co(sep)^{3+}$–Mag(100°C) ($Q^3/Q^4 = 0.26$). These data confirmed that the layer structure of magadiite remained intact after intercalation of $[Co(sep)]^{3+}$. Earlier workers have published Q^3/Q^4 ratios for Na^+-magadiite that range from 0.25–1 [2, 15, 18]. However, a careful evaluation of the relaxation times for the various ^{29}Si environments has not been undertaken until now. We have found that the spin-lattice relaxation times for the Q^3 site is 160 s and ≈ 280 s for the Q^4 sites. The differences in Q^3 and Q^4 relaxation times can be

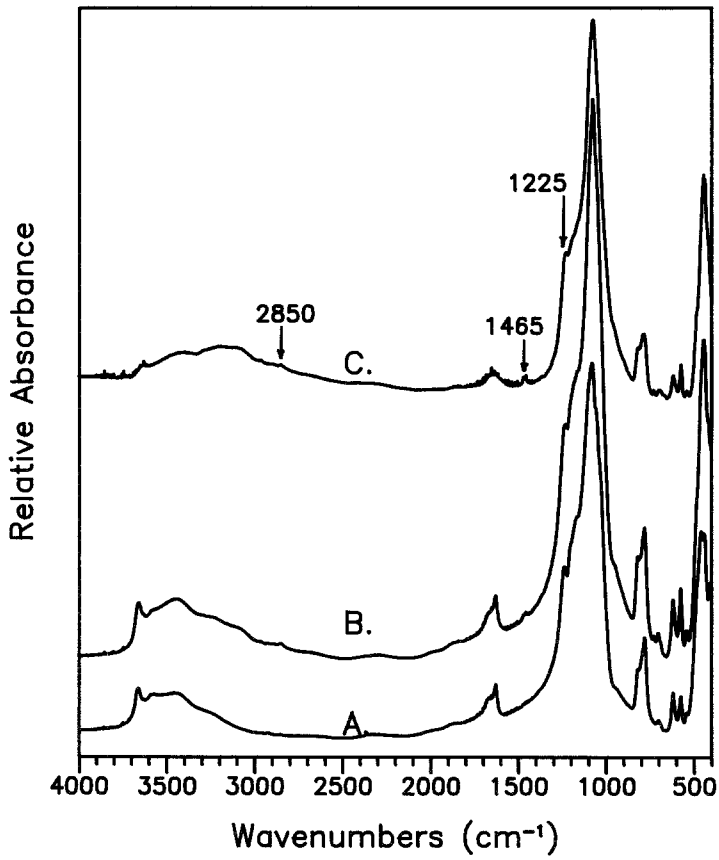

Fig. 7. Infrared spectra (2% w/w KBr pellet) of (A) Na^+-magadiite, (B) $Co(sep)^{3+}$–mag(25°C), and (C) $Co(sep)^{3+}$–mag(100°C).

attributed to the presence of H_2O in the interlayer. The importance of $^{29}Si-^1H$ dipolar relaxation via water molecules has been shown for other layered materials [19]. The close proximity of interlayer water to the Q^3 ^{29}Si sites of Na^+-magadiite allows for their relaxation via $^{29}Si-^1H$ dipolar relaxation and, in turn, reduces the relaxation time of the Q^3 site greatly as compared to the Q^4 site.

Infrared spectra for Na^+-magadiite and the $Co(sep)^{3+}$ reaction products are shown in Figure 7. The IR spectrum for Na^+-magadiite, Figure 7(c), agreed well with those reported elsewhere [15, 20]. The bands centered at 3500 cm^{-1} and 1650 cm^{-1} were assigned to the stretching and bending frequencies, respectively, of intercalated water. The bands from 1500–400 cm^{-1} have been attributed to the stretching and bending frequencies of the SiO_4 units that make up the layer. Garces *et al.* [15] have assigned the bands at about 1225 cm^{-1} to five membered rings of SiO_4 tetrahedra, which are known to be present in certain zeolites.

The IR spectrum of $Co(sep)^{3+}$–Mag(100°C) exhibited all the peaks characteristic of magadiite, along with peak absorptions from $Co(sep)^{3+}$. Weak broad IR bands at 3100 cm^{-1}, 2960 cm^{-1} and 2850 cm^{-1} were assigned to the C—H stretch-

ing frequencies of the ligand. Also, a weak absorption at 1465 cm^{-1} was characteristic of the C—H asymmetric bending modes of $Co(sep)^{3+}$. The characteristic magadiite absorptions in the 1500–400 cm^{-1} region remained unchanged upon intercalation of $Co(sep)^{3+}$ cation, indicating that the layered structure was not changed during intercalation.

Nitrogen adsorption isotherms over the partial pressure range of $0 < P/P_0 < 0.4$ were obtained at −196°C for Na^+-magadiite, and the $Co(sep)^{3+}$ reaction products. The data were treated using the BET equation [12] in order to obtain surface area values. The equivalent surfaces areas were determined from the BET monolayer volume V_m (BET), and the microporous volumes determined from the *t*-plots (see Table III). A very small microporous surface area, (7 m^2/g), was observed for $Co(sep)^{3+}$–Mag(25°C). The virtually non-existent microporosity was consistent with little or no $Co(sep)^{3+}$ intercalation for the reaction product obtained at 25°C. Somewhat more surprising was the low microporous surface area for $Co(sep)^{3+}$–Mag(100°C), (8.7 m^2/g). Although $Co(sep)^{3+}$ had been intercalated, apparently insufficient space was available to allow access to the nitrogen molecule (kinetic diameter 3.6 Å). That is, the mixed $Co(sep)^{3+}$ and Co^{2+} intercalation product appeared to be 'stuffed' with little free volume between the metal complex pillars.

Na^+-magadiite is known to adopt a particle morphology composed of silicate layers intergrown to form spherical nodules resembling rosettes [15]. The proton exchange form of magadiite also has this characteristic particle morphology [7]. Scanning electron micrographs of the $Co(sep)^{3+}$ reaction products, shown in Figure 8b and 8c, revealed the same morphology as the starting Na^+-magadiite, Figure 8a, except that the size of the rosettes were reduced by the attrition caused by vigorous stirring during reaction. This result indicated that the $Co(sep)^{3+}$ in $Co(sep)^{3+}$-magadiite(100°C) was intercalated in a topotactic fashion. Close inspection of the micrographs also indicated the absence of other crystalline phases.

The demetalation of $Co(sep)^{3+}$ that occurred upon reaction of the complex with Na^+-magadiite at 100°C is particularly noteworthy. Sargeson and this coworkers have reported previously that it was not possible to remove the metal from the Co(III) complex [11]. $Co(sep)^{3+}$ is very stable and remains intact even after prolonged treatment in boiling 12 M HCl. Elemental analyses suggested that during the intercalation of $Co(sep)^{3+}$, one half of the metal centers were no longer complexed by the sepulchrate ligand. This was confirmed by qualitative analysis for

Table III. Surface area analysis of intercalated derivatives

Sample	S_{BET} m^2 g^{-1}	V_m cm^3 liq g^{-1}	Nonmicroporous Surface m^2 g^{-1}
Na^+-magadiite	24	0	24
H^+-magadiite	45	0	45
$Co(sep)^{3+}$–Magadiite (25°C)	33	0.0025 (7 m^2 g^{-1})	24
$Co(sep)^{3+}$–Magadiite (100°C)	57	0.0031 (8.7 m^2 g^{-1})	48

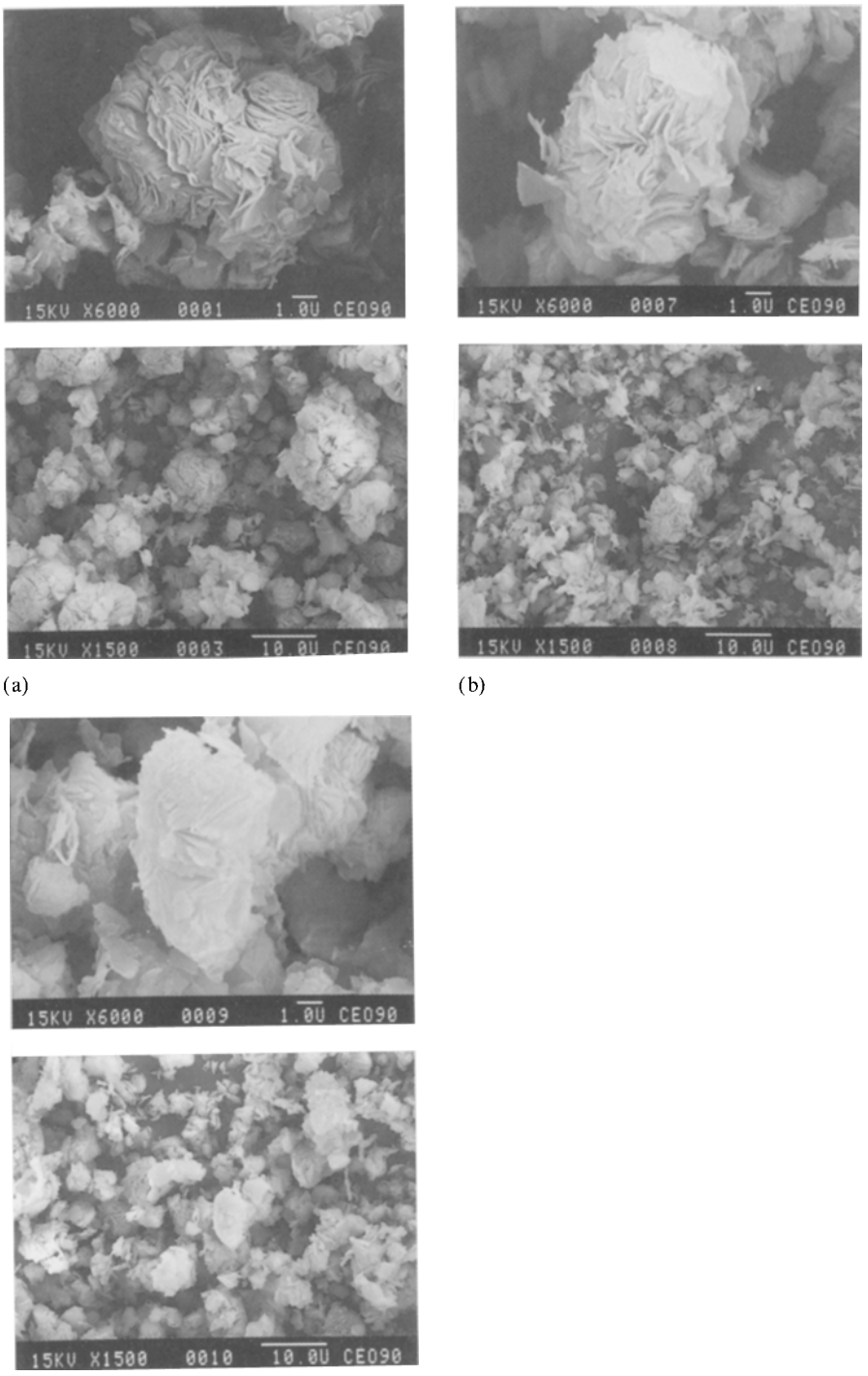

Fig. 8. Scanning electron micrographs at × 6000 and × 1500 magnification for (a) Na^{+}-magadiite, (b) $Co(sep)^{3+}$–mag(25°C), and (c) $Co(sep)^{3+}$–mag(100°C).

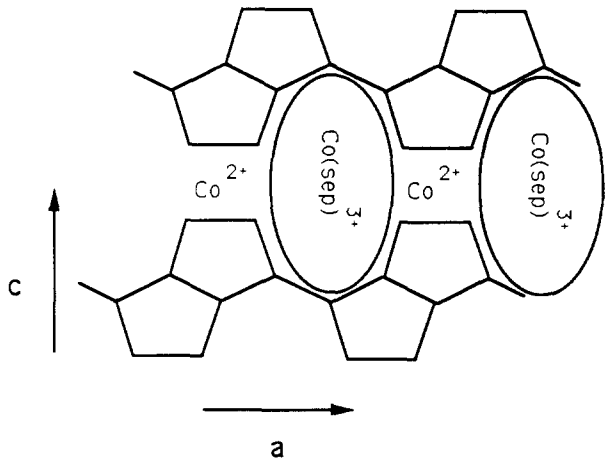

Fig. 9. Proposed positions of $Co(sep)^{3+}$ ions in the pleated folds of magadiite. Co^{2+} cations are placed at the ridges which form between folds. Vertices of the magadiite layer represent silicon positions; oxygen positions are between adjacent silicon pairs. The fourth coordination position of silicon is not shown.

Co(II). The stability of $Co(sep)Cl_3$ was tested in basic solution under reaction conditions identical to those used to obtain the 100°C intercalation product. Under these conditions no Co(II) was detected using the SCN^- qualitative test. Demetalation seemed to be a direct result of the interaction of $Co(sep)^{3+}$ with magadiite. It has been shown that treatment of $Co(sep)^{2+}$ with acid leads to release of Co(II) from the sepulchrate ligand [11], but an analogous reaction does not occur for the 3^+ cation. The mechanism of decomplexation on the magadiite surface may have involved reduction of the $Co(sep)^{3+}$ complex by water followed by rupture of the cage and release of Co(II). The oval shaped $Co(sep)^{3+}$ is oriented with its long axis parallel to the silicate sheet, as judged from the 6.4 Å gallery height obtained by X-ray diffraction. Magadiite might facilitate the reduction of $Co(sep)^{3+}$ by distorting the bicyclic complex in the intercalated state.

The relatively sharp X-ray diffraction pattern observed for $Co(sep)^{3+}$-magadiite(100°C) indicated that the material was regularly intercalated. That is, both the $Co(sep)^{3+}$ and Co^{2+} cations appear to be mixed within each interlayer in a uniform manner. A previously proposed model structure for Na^+-magadiite suggested that the magadiite layer has a corrugated surface [15]. A plausible arrangement in this case could involve placement of the larger $Co(sep)^{3+}$ cations between the pleated folds of the layer with the Co^{2+} cations adopting positions at the ridges as illustrated in Figure 9. Confirmation of this structure will have to await future studies of the magadiite structure.

4. Conclusions

The reaction of $Co(sep)^{3+}$ with Na^+-magadiite at 25°C resulted in a product that contained $Co(sep)^{3+}$ cations bound to the external crystallite surfaces of the layered silicate. In contrast, reaction at 100°C resulted in penetration of the metal

complex between the layers of magadiite. The magadiite structure was retained even after prolonged reaction with $Co(sep)^{3+}$ at 100°C. Moreover, the particle morphology for the $Co(sep)^{3+}$ intercalated derivative was the same as the starting Na^+-magadiite suggesting a topotactic was the partial demetalation of $Co(sep)^{3+}$ which resulted in a mixed ion intercalate containing both Co^{2+} and $Co(sep)^{3+}$ between the layers. N_2 surface area analysis indicated that only a small amount of microporous surface existed in the $Co(sep)^{3+}$ intercalated derivative, indicating that most of the interlayer space was stuffed with little or no available microporosity between pillars. Thus, $Co(sep)^{3+}$ is not suitable for the pillaring of magadiite, even though this cation has been successfully used previously as a pillaring agent for related ionic structures such as smectite clays [16]. In the case of the layered sodium silicates it seems that pillaring is difficult to achieve by direct ionic exchange. Future work will focus in part on the use of robust organic cation intercalated derivatives of magadiite for accessing the intracrystalline space of magadiite by organic molecules from aqueous solution.

Acknowledgement

This research was supported in part by NSF grant DMR 89-03579 and the Michigan State University Center for Fundamental Materials. J. S. D. wishes to acknowledge a student training stipend under NIEHS grant 1P42ESO4911-01.

References

1. I. V. Mitchell (ed.): *Pillard Layered Structures*: *Current Trends and Applications*, Elsevier, New York (1990).
2. T. J. Pinnavaia, I. D. Johnson and M. Lipsicas: *J. Solid State Chem.* **63,** 118 (1986).
3. H. P. Eugster: *Science* **157,** 1177 (1967).
4. R. A. Fletcher, and D. M. Bibby: *Clays Clay Miner.* **35,** 318 (1987).
5. K. Beneke and G. Lagaly: *Am. Miner.* **68,** 818 (1983).
6. K. Beneke and G. Lagaly: *Am. Miner.* **62,** 763 (1977).
7. G. Lagaly and K. Beneke: *Am. Miner.* **60,** 642 (1975).
8. T. Yanagisawa, K. Kuroda, and C. Kato: *Reactivity of Solids* **5,** 167 (1988).
9. M. M. Mortland, S. Shaobai and S. A. Boyd: *Clays Clay Miner.* **34,** 581 (1986).
10. S. A. Boyd, S. Shaobai, J. F. Lee, and M. M. Mortland: *Clays Clay Miner.* **36,** 125 (1988).
11. I. I. Creaser, R. J. Geue, J. MacB. Harrowfield, A. J. Herlt, A. M. Sargeson, M. R. Snow, and J. Sprinborg: *J. Am. Chem. Soc.* **104,** 6016 (1982).
12. S. J. Gregg, and K. S. W. Sing: *Adsorption, Surface Area and Porosity*, 2nd edition, Academic press, London (1982).
13. G. W. Brindley: *Am. Miner.* **54,** 1583 (1969).
14. J. L. McAtee, R. House, H. P. Eugster: *Am. Miner.* **53,** 2061 (1968).
15. J. M. Garces, S. C. Rocke, C. E. Crowder, D. L. Hasha: *Clays Clay Miner.* **36,** 409 (1988).
16. F. Tsvetkov and J. White: *J. Am. Chem. Soc.* **110,** 3183 (1988).
17. W. L. Masterton, E. J. Slowinski, and C. L. Stanitski: *Chemical Principals*, Alternate Edition, 5th edition, CBS College Publishing (1983).
18. W. Schwieger, D. Heidemann, and K. Bergk: *Rev. Chim. Min.* **22,** 639 (1985).
19. P. F. Barron, P. Slade, and R. L. Frost: *J. Phys. Chem.* **89,** 3305 (1985).
20. J. M. Rojo, E. Ruiz-Hitzky and J. Sanz: *Inorg. Chem.* **27,** 2785 (1988).